A Review: Crotalaria Verrucosa, Acalypha Indica Leaf Extract Mediated Synthesis Of Zinc Oxide Nanoparticles.

A project Report submitted in partial fulfillment of the requirement for the Fourth semester of the Degree of Master of Science in Chemistry

SHIVAJI UNIVERSITY, KOLHAPUR

SUBMITTED BY

Mr. VISHAL BHIKAJI NAIK

Mr. SATYAJIT MADHUKA LOHAR

Mr. HARSHAD VISHNU KUMBHR

Under the Guidance of

Prof. NILKHANT BHOSALE M. Sc., NET

Department of Chemistry

SHIVARJ COLLEGE GADHINGLAJ

2020-2021

CERTIFICATE

CERTIFIED THAT PROJECT WORK COMPLETED

Crotalaria Verrucosa, Acalypha Indica Leaf Extract Mediated Synthesis Of Zinc Oxide Nanoparticles.

By

Mr. VISHAL BHIKAJI NAIK

Mr. SATYAJIT MADHUKA LOHAR

Mr. HARSHAD VISHNU KUMBHR

In partial fulfillment for the fourth semester of Master of Science in chemistry of the Shivaji University, Kolhapur During the year 2020-2021. It is certified that all Correction /suggestion Indicated for internal assessment have been incorporated in the report deposited in the departmental library. The project has been approved as it satisfies the academic requirements in aspects of project work prescribed for the Master of Science Degree.

Sign of the Guide

Prof. NILKHANT BHOSALE

Sign of the H.O.D.

Prof. S.D. PATIL

Examiners Sign.

ACKNOWLEDGEMENT

It gives us an immense pleasure to write an acknowledgement to this Project report, a contribution of all people who helped us realize it. Also we express our deep sense of gratitude and appreciation to our beloved H.O.D. Prof. S. P. Chavan for this enthusiastic inspiration and amicable in all phases of our project

With due respects we would like to express our sincere thanks to our project Guide Prof. Sudhir Kurade for his sterling efforts and timely guidance, patience in solving our doubts, which kept cropping up in due course of our project work needs special credits .

Lastly, I'm very much indebted to My Dear Parents who helped me in all the steps of my career & also would like to thank My Friends for their cooperation & help.

Yours Sincerely

Mr. VISHAL BHIKAJI NAIK

Mr. SATYAJIT MADHUKA LOHAR

Mr. HARSHAL VISHNU KUMBHR

DECLARATION

I declare that this dissertation entitled **"Crotalaria Verrucosa, Acalypha Indica Leaf Extract Mediated Synthesis of Zinc Oxide Nanoparticles".**

is the result of my own work except as cited in the references.the dissertation has not been accepted for any degree and is not concurrently submitted in canditure of any other degree.

Signature :

Name of candidate : VISHAL BHIKAJI NAIK.

Date :

INDEX

Sr.No.	Perticulars	Page No.
1.	Submission Report	1
2.	Certificate	2
3.	Acknowledgements	3
4.	Declaration	4
5.	INDEX	5
6.	Abstract	6
8.	Introduction	7-10
9.	Synthetic Method	11-18
10.	Result & Discussion	19
11.	Synthesis And Characterisation	19-31
11.	Conclusion	32
12.	References	33-37

ABSTRACT

In this work, we present an ecofriendly, non-hazardous, green synthesis of zinc oxide nanoparticles (ZnO NPs) by leaf extract of Crotalaria verrucosa (C. verrucosa). Total phenolic content,total flavonoid and total protein contents of C. verrucosa were determined. Further, synthesizedZnO NPs was characterized by UV–visible spectroscopy (UV-vis), X-ray diffractometer (XRD),Fourier transform infra-red (FTIR) Spectra, transmission electron microscope (TEM), and Dynamiclight scattering (DLS) analysis. UV-vis shows peak at 375 nm which is unique to ZnO NPs.XRD analysis demonstrates the hexagonal phase structures of ZnO NPs. FTIR spectra demonstratesthe molecules and bondings associated with the synthesized ZnO NPs and assures the role ofphytochemical compounds of C. verrucosa in reduction and capping of ZnO NPs. TEM imageexhibits that the prepared ZnO NPs is hexagonal shaped and in size ranged between 16 to 38 nmwhich is confirmed by DLS. Thermo- gravimetric analysis (TGA) was performed to determinethe thermal stability of biosynthesized nanoparticles during calcination. The prepared ZnO NPsshowed significant antibacterial potentiality against Gram-positive (S. aureus) and Gram-negative(Proteus vulgaris, Klebsiella pneumoniae, and Escherichia coli) pathogenic bacteria and SEM imageshows the generalized mechanism of action in bacterial cell after NPs internalization. In addition,NPs are also found to be effective against the studied cancer cell lines for which cytotoxicity wasassessed using MTT assay and results demonstrate highest growth of inhibition at the concentrationof 100
g/mL with IC50 value at 7.07g/mL for HeLa and 6.30g/mL for DU145 cell lines, in contrastto positive control (C. verrucosa leaf extract) with IC50 of 22.30 g/mL on HeLa cells and 15.72 g/mL
on DU145 cells. Outcome of the synthesized ZnO NPs using C. verrucosa shows antimicrobial activity against studiedmicrobes, also cytotoxicity, apoptotic mediated DNA damage and antiproliferative potentiality inthe studied carcinoma cells and hence, can be further used in biomedical, pharmaceutical and foodprocessing industries as an effective antimicrobial and anti-cancerous agent.

ZnO nanoparticles were green-synthesized from Acalypha indica leaf extract using zinc acetate as a precursor. The prepared ZnO nanoparticles were calcined at three different temperatures, namely 100, 300, and 600 °C. The structure/morphology of the green-synthesized ZnO nanoparticles was ascertained through X-ray diffraction, particle size analysis, scanning electron microscopy, transmission electron microscopy, and surface area analysis techniques. It was observed from the physico-chemical and biological characterization studies that ZnO nanoparticles calcined at high temperature (600 °C) exhibit high surface area ($230^2/g$) and small particle size (20 nm) with good antibacterial activity againstEscherichia coli (22.89 ± 0.06 mm) and Staphylococcus aureus (24.62 ± 0.08 mm). In addition, cotton fabrics coated with these nanoparticles showed higher UV-protection (87.8 UPF), hydrophobicity (155_), and maximum zone of bacterial inhibition against E. coli and S. aureus (25.13 ± 0.05 mm and 30.17 ± 0.03 42
mm) than those coated with particles calcined at 100 °C and 300 °C. High temperature calcination has a vital role in the crystallization of the particles towards nanoscale with increased resistivity to UV exposure, washing treatments, and microbial infection in fabrics. Thus, the cost-effective ZnO nanoparticles obtained through green synthesis method proves their potential applications in the field of biomedical,textile, and cosmetic applications.

Keywords: ZnO NPs; C. verrucosa; A.indica; characterization; antimicrobial activity; antibacterial activity; anti-cancerous potentiality; hydrophobici

INTRODUCTION

Nanotechnology is the greatest dynamic area of exploration in modern material science and has established as the great innovation of things at the nanoscale of 1 to 100 nm. Nano is a Greek word symbolizing “dwarf” in the one-billionth scale (10-9). To synthesis nanomaterial of various shapes and dimensions, two different methods of approaches have been widely used namely bottom-up and top-down approaches.
Building up of nanomaterials from an atom by atom is a bottom-up approach while trimming down bulk material to smaller nano size is a top-down approach. Nano is a metric measure of one billionth of a meter and covers a width of 10 atoms. In terms of comparison with real objects, an example that hair is 150,000 nanometers may be given. The rapidly developing nanotechnology is the inter-disciplinary research and development field of biology, chemistry, physics, food, medicine, electronics, aerospace, medicine, etc., which examines the design, manufacture, as-sembly, characterization of materials that are smaller than 100 nanometers in scale, as well as the application of minia-ture functional systems derived from these materials. It rep-resents the whole of development activities. As fır the nano-biotechnology, on the other hand, it is the result of a combi-nation of biotechnology and nanotechnology branches with a common combined functioning.
NPs re virtualized in its application by its dimension, shape, morphology and size (Vijayaraghavan et al. 2012, Khin et al. 2012, Dimkpa et al. 2012 and Ain et al. 2013) It can be one dimensional (1D), 2D or 3D. NPs used in electronic gadgets and sensing devices are thin-film 1D. 2D carbon nanotubes (CNTs) have more application in the field of catalysis because of its stableness and a high degree of adsorption. Quantum dots and clusters are grouped as 3D NPs. Metal NPs like Ag, Au, Pd, Pt, Zn, Fe are mainly formed from its salt solutions like AgNO3, AuCl4, PdCl4, PtCl4, ZnSO4 by physical and chemical methods. Based on its chemical nature NPs are grouped as metals, metal oxides, silicates, non-oxide ceramics, polymers, organics, carbon and biomolecules. Correct exploitation of ecologically benevolent solvents and nontoxic chemicals are some of the core subjects in the green synthesis approach contemplations. This review implies the importance of green synthesis of metal NPs in a benign greener way following the 12 principles of green chemistry without defiling the environment.

Nanoparticles (NPs) are the engineered assemblage of materials having nanoscale dimensions with a size distribution range of 1–100 nm diameters as defined by the National Nanotechnology Initiative (NNI), with unique physicochemical properties due to their nanosize, hydrophilic and hydrophobic nature, functional moieties on surface, high surface to volume ratio and aggregation properties [1].
Nanoparticles permit precision engineering to track and regulate their interaction with biological systems and hence nanotechnology integrated with biology is now very much involved in the creation of modern and more effective antimicrobial and anticancerous agents. Metal oxide nanoparticles provide promising and wide perspectives for biomedical fields through the production of nanomaterials,notably antimicrobial, anticancerous drugs, gene delivery, cell imaging, and biosensing [2]. Bacterialinfections are considered to be a significant health issue on a global level. Mutations in bacterial genesand multiple drug resistance (MDR) have raised challenges to treat MDR microorganisms becauseresistance drastically restricts therapeutic options and hence there is a need for e_ective antibacterialagents without adverse e_ects on treated cells. ZnO NPs are e_cient multifunctional inorganicmetal oxide NPs that have a wide energy gap of 3.37 eV with short wavelength and large excitonbinding energy of 60 meV, is considered to be moderately toxic but is extremely reactive and sensitivewith extreme absorbent potentiality [3]. ZnO NPs have been given considerable attention by variedapplications in terms of their antimicrobial properties thereby reducing the problem of

multi-drugresistance. Zinc is considered to be a significant trace element in tissues of the body, such as brain,muscle, bone, and skin, maintaining many physiological functions and without which few enzymesnamely carbonic anhydrase, carboxypeptidase, and alcohol dehydrogenase become quiescent [4].

Being a central component of di_erent enzymes, zinc is involved in body metabolism and plays a vital role in hematopoiesis, synthesis of proteins and nucleic acid [5–7]. While, the eukaryotes are found resistant to lower concentrations of zinc oxide NPs [8]. Interestingly, nanosized ZnO is classified and recognized as safe (GRAS) by the US Food and Drug Administration (FDA) [9].

Crotalaria verrucosa L. plant belongs to family Papilionaceae, commonly known as blue rattlepod, Kilukiluppai, and Ghelegherinta, is a small shrub broadly distributed all over India, from the Himalayas to Ceylon [31]. This plant is generally cultivated as manure in improving soil quality for vegetation [32]. The leaf extract was used in traditional medicine against several diseases such as rheumatism, skin allergies, tetanus, salviations, biliousness, scabies, impetigo, dyspepsia, diarrhoea, jaundice, cardiac abnormalities, fever, dysentery, and leprosy [33–36] which is due to presence of bioactive compounds.. Previous literature stated that the leaf extract of C. verrucosa contains alkaloids,flavonoids, glycosides, tannins, steroids, polyphenolic compound, among others, and majorly alkaloids,flavonoids, tannins, and terpenoids reported to show significant cytotoxicity on cancer cell [37,38].Ahmed et al. [39] manifested that leaf extract of C. verrucosa is e_ectively cytotoxic particularlyagainst cervical HeLa cells due to (+) -Catechin hydrate and (+)-Epicatechin (tannins) compound which is responsible for its anticancer potentiality. Flavonoids due to presence of hydroxyl group act as antioxidants by preventing or neutralizing the free radical formation in the body [40,41]. Thus,investigation aimed to synthesize ZnO NPs using C. verrucosa to evaluate the antibacterial, cytotoxic and anticancerous potency. Therefore, the study has designed to synthesize and characterize ZnO NPs using C. verrucosa leaf extracts which would be eco-friendly, non-toxic and endowed with the antimicrobial activity against pathogens as well as anticancerous properties. The concept of our work is shownin Figure 1. The complex architecture of secondary plant metabolites are involved in nanoparticle synthesis and have shown to contribute in multi-target e_cacy. Because of the complexities of cancer,a novel, multi-targeting bioactive compound is the need of the time. One potential cause may be the modulatory effect of the phytoconstituents on apoptosis which incomparison to normal cells is often blocked in cancer cells.

Figure 1. Schematic illustration of the biological synthesis of ZnO NPs using Crotalaria verrucosa leaf extract and its applications.

Zinc oxide (ZnO) nanoparticles are nowadays used in textile industries due to their white appearance, less cost, UV-shielding property, and antibacterial activities [1–3]. ZnO nanoparticles are reported to possess the ability to inhibit the growth of both gram-positive and gram-negative bacteria [4]. These nanoparticles inhibit the bacterial growth through different mechanisms such as cell membrane penetration, attachment on bacterial surface via electrostatic forces and damage the cell wall, and production of reactive oxygen species [5–7]. These nanoparticles find potential technological applications such as protection of the body against solar radiation and bacterial infections [8].The ZnO nanoparticles are conventionally synthesized using many physical and chemical methods. The physical methods such as metal-organic chemical vapor deposition, sputtering technique,
pulsed laser deposition, infrared irradiation, thermal decomposition, thermal evaporation, and condensation are extensively used to synthesize ZnO nano particles [6–10]. The chemical route method, which requires high vacuum and energy, includes liquid ultra sonication, sol–gel, and electrochemical reaction methods [11–14]. These methods consume more energy and hazardous chemical reagents, which may be hazardous in nature and may yield by-products of non-eco-friendly nature [15]. Green synthesis of nano particles can overcome the problems related to physical and chemical methods. Moreover, green synthesis method does not require any harmful chemicals as reducing and oxidizing agents since it requires only plant extracts

[16,17]. Green synthesis of nanoparticles using plant extracts is one of the cleanest, biocompatible, non-toxic, and ecofriendly methods for large-scale production of nanoparticles [18–20]. The main component present in plant extracts, namely polyol, acts as a chelating and capping agent for rapid biosynthesis of nanoparticles and stabilizes the formation of metallic nanoparticles [21]. The majority of review supports that metal oxide nanoparticles such as silver, ferric, copper, gold, and palladium are synthesized via
green synthesis route, with excellent structure/morphology and better physico-chemical properties [22–25].Extracts from different plants such as Agathosma betulina, Aspa-lathus linearis, Durantaerecta, Peperomia pellucida L., and Celosia argentea are used for the synthesis of ZnO nanoparticles [26–29].

Acalypha indica is a common weed that belongs to the Euphorbiaceae family. The leaves of A. indica have already been evaluated for their wound-healing activity in pets [30]. Attempt has been made to cure diseases such as pneumonia, asthma, and rheumatism using the ZnO nanoparticles obtained from A. indica plant leaves [31]. Dried A. indica leaves are used to reduce bedsore by placing them on bed surface, whereas the extract from the plant leaves is mixed with oil or lime and then, used to cure many skin diseases [31]. The textile products, especially those made from natural fibers, provide an excellent environment for microorganisms to grow, because of their large surface area and ability to retainmoisture. Most textile materials currently used in hospitals and hotels are known to cause cross-infection and transmission of diseases caused by microorganisms. There are different physicochemical methods that can be considered for the production of antimicrobial fabrics. Antimicrobials are used as bacteriostatic, bactericidal, fungistatic and fungicidal activities, and offer special protection against various forms of textile rotting [32–34].

Bio nanocomposites are components of natural polymer matrix mixed with organic/inorganic metal particles at nanoscale [35].In our earlier studies, chitosan–ZnO nanocomposite particles are used for UV-protection and antibacterial finishing on textile fabrics[36,37]. Theproperties such as biocompatibility, biodegradability,microbial protection, high permeability, and non-toxic nature ofchitosan are considered positively and hence, used for many industrial applications [38–40]. The effect of processing temperature on the formation of ZnO nanostructure with optimized physicochemical as well as biomedical properties is found to be scanty.The objective of the present work is to synthesize ZnO nanoparticles employing green synthesis approach from the leaf extract of A. indica and zinc acetate precursor. The prepared ZnO nanoparticles effectively coated on cotton fabrics and then, its functional properties like UV protection, hydrophobicity and antibacterial behaviours are explored. The present study is mainly aimed to provide an excellent textural property by coating the optimized ZnO nanoparticles on the fabrics. In addition, use of green synthesized ZnO nanoparticles to enhance the functional properties of cotton fabrics is one of the fascinating emerging researches in medical textiles.

SYNTHETIC METHODS

.

3.1. Chemicals and Reagents
Zinc nitrate [Zn(NO3)2_6H2O] was purchased from Merck, Mumbai, India. Meuller–Hinton agar (MHA), 3-[4,5-96dimethylthiazole-2-yl]-2,5-diphenyltetrazolium bromide (MTT), DAPI (40,6-diamidino-2-phenylindole) and Dulbecco's modified Eagle medium (DMEM) were obtained from Sigma-Aldrich and Himedia Laboratories. All the chemicals and reagents used in this study were graded with analytical reagents (AR) and the experiments involved in this study were done using milli-Q and sterile distilled water.

3.2. Preparation of Leaf Extract and Phytochemical Analysis
Leaves of C. verrucosa was collected from Sri Venkateswara University, Tirupathi, India and the plant species was identified and authenticated by an expert taxonomist Dr. Madhava Chetty, Assistant Professor at Department of Botany, Sri Venkateswara University, Tirupati. The collected fresh leaves of C. verrucosa were cleaned considerably with cool running tap water followed by milli-Qwater. The washed leaves were then dried in the shade for 12–14 days until all the humidity had been lost, then grounded to powder in clean grinder. Ten grams of powdered leaves was weighed and boiled in Erlenmeyer flask containing 100 mL milli-Q for 10 min at 70 _C and allowed to cool at room temperature. The aqueous portion was then filtered via Whatman No. 1 filter paper and stored it at 4 ℃ in storage vials for further experimental usage. The bioactive compounds in the leaf extract were analyzed because these phytochemicals can act as stabilizing and reducing agents in the green synthesis of metal oxides. Remaining dried leaves were placed in an airtight vessel at normal temperature for consequent extract mediated NPs preparation.

3.2.1. Total Phenolics

The total phenolic content in C. verrucosa leaf extract was estimated with the Folin–Ciocalteu method [83]. The extract of 140 mL (1 mg/mL) was mixed to react with 600 mL of Folin–Ciocalteu reagent (0.2 M) for 5min followed by the addition of 460 mL sodium carbonate (7.5%). The integral setup was incubated at 45 ℃ for 30 min followed by 1 h at room temperature in dark. The absorbance was measured at 650 nm (considering gallic acid as standard), calculated from calibration curve and outcome were presented as mg of gallic acid equivalents per gm (GAE/gm) of extract.

3.2.2. Total Flavonoid Content

A colorimetric aluminium chloride (AlCl3) approach is used to estimate the total flavonoid contents of crude extract following Chang et al. [84]. Briefly, 25 mL (1 mg/mL) of the extract was added to 75 mL of methanol and the final volume was made upto 2 mL with distilled water. To this, 300 _L of 5% sodium nitrate and 300 _L of 10% AlCl3 were added followed by incubation of 10 min. Then 2 mL of 1 mol/L NaOH was added to the solution and final volume was adjusted upto 5 mL by using distilled water and allowed the solution to incubate for 40 min at room temperature and the OD was recorded at 510 nm. Results calculated from a calibration curve taking rutin as standard, and values were expressed as mg of Rutin equivalents per gram (mg RE/gm) of extract
.

3.2.3. Determination of Proteins

Total proteins in leaf extract were measured using the Biuret test by treating the extract with 1 mL (10%) of sodium hydroxide solution followed by heating. A drop of copper sulfate solution (0.7%) was mixed with the solution and incubated at room temperature for 30 min leading to the formation of purplish violet color and the OD was measured at 540 nm. Bovine serum albumin (BSA) was kept as standard and results are given as mg of BSA per gm of the sample.

3.2.4. FTIR Spectrum Analysis of C. verrucosa Leaf Extract

Leaves of C. verrucosa were weighed and mixed with KBr salt forming a compressed pellet and was examined in FTIR spectroscope. Results were recorded using Perkin Elmer FTIR Frontier Spectrophotometer in the range of 4000–400 cm-1.

3.3. Green Synthesis of ZnO NPs

About 20 mL of C. verrucosa leaf extract (1 mg/mL) was taken in 250 mL Erlenmeyer flask and 2 gm of Zn(NO3)2.6H2O was added. For the purpose, 20 mL of plant extract was heated at 60 ^{0}C under continuous stirring in the presence of sunlight, followed by the addition of 2 gm of zincnitrate. The mixture of the solution was continuously stirred until yellow color paste was obtained.
The precipitate was calcinated at 400 ^{0}C for 3 h. Finally, white powder was obtained and used it for further analysis.

2.1. Sample collection

Fresh leaves of A. indica were collected from in and around Bhudergad, Maharashtra,India. The collected leaves were washed twice with tap water, followed by washing through doubledistilled (DD) water for multiple times to remove dust particles from the surface of the leaves. The washed leaves were shade dried for 15 days.

2.2. Preparation of leaf extract

The dried A. indica leaves were subjected to ball milling for 15 h and then, a fine leaf powder was obtained. To prepare the leaf extract, 2 g of fine leaf powder was dissolved in 100 ml DD water and then, stirred for 2 h at a constant temperature of 70ºC. This mixture was cooled to room temperature and was filtered using Whatman (No. 3) filter paper. The obtained leaf extract was used as a catalyst to synthesize ZnO nanoparticles without adding any other chemicals.

2.3. Preparation of ZnO nanoparticles

The prepared 50 ml of A. indica of leaf extract was added with 0.5 g of 1 M (Merck, 99.9%) zinc acetate under stirring for 1h at 60ºC. The obtained precipitate was washed with DD water for several times and then, finally heated in a hot-air oven at 80ºC for 24h. The obtained ZnO nanopowders were calcined at three different temperatures, namely 100, 300, and 600ºC. These calcined ZnO nanopowders at 100, 300, and 600 ºC are hereafter termed as Zn100, Zn300, and

Zn600, respectively. The schematic representation of ZnO nanoparticles synthesis procedure is shown in Fig. 1.

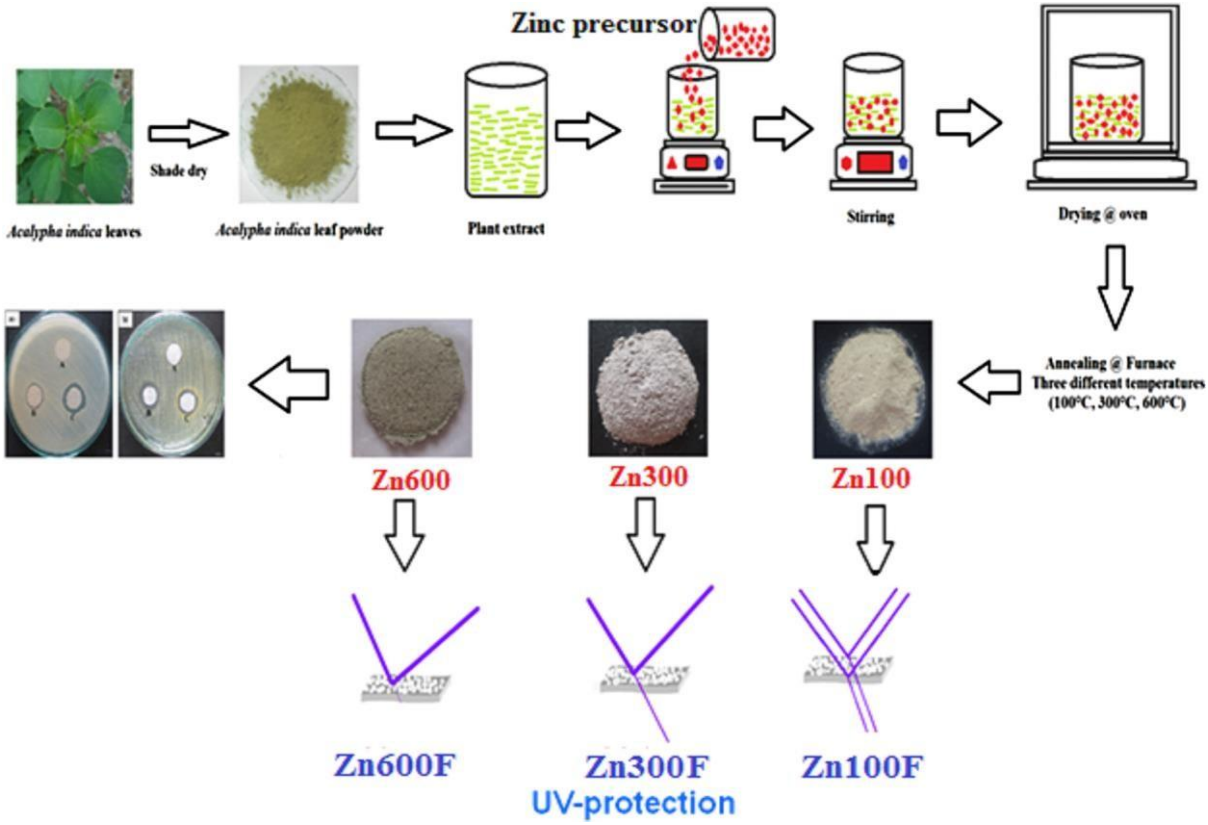

2.4. Characterization of ZnO nanoparticles synthesis

The X-ray diffraction (XRD) pattern of the prepared Zn100, Zn300, and Zn600 nanoparticles were obtained using a Philips X'Pert MPD powder diffractometer (X'Pert PRO;PANalytical, The Netherlands) operated with a long fine focus of Cu anode at 40kV and 30 mA in Bragg–Brentano geometry. The XRD pattern was obtained in the 2Θ range from 10º to 80º in a step-scan mode with 2Θ step size of 0.02º. The purity of the prepared ZnO nanoparticles was identified using an X-ray fluorescence spectrometer (EDX- 720; Shimadzu, Japan). The UV–visible spectra of all the prepared ZnO nanoparticles were recorded using a UV–visible spectrophotometer (Cary 8454; Agilent, Singapore) operated in the UV to near-IR (180–800 nm) spectral region. A submicrometer particle size analyzer (Nanophox; Sympatec,Germany) using a dynamic light scattering technique was used to determine the particle size. The size of all ZnO nanoparticles was measured in the range of 1–1000 nm at a scattering angle of 90º. A three-point BET plot was derived from a surface area analyzer (Autosorb AS-1MP; Quantachrome, Boynton Beach, FL) to determine the surface area of the prepared Zn100, Zn300, and Zn600 nanoparticles. The morphology, microstructure, and elemental composition of all the samples were analyzed using a scanning electron microscope

coupled with Energy-dispersive X-ray analysis (JSM 6360; JEOL, Japan). A transmission electron microscope (TEM, CM200; Philips, Eindhoven, The Netherlands) operated at a potential of 120 kV was used to obtain TEM image and then, to determine the crystallite size and surface morphology of all ZnO nanoparticles. The average particle size and diffraction pattern of the ZnO nanoparticles were determined.

2.5. Nanocomposite coating on cotton fabrics

The chitosan solution was prepared by dissolving 1 g chitosan in 1M acetic acid with 1 L DD water under stirring for 12 h at 80ºC. The ZnO nanoparticles (2 g) were mixed with the prepared chitosan solution to prepare the ZnO nanocomposite. This mixture was stirred for 1 h and 30min, and then, sonicated. The obtained homogeneous ZnO nanocomposite mixture was coated on a 100% fabric is termed as UC-CF and also considered as the reference, to explore the changes in the functional properties of ZnO nanoparticles-coated fabrics. The fabrics after coating with Zn100, Zn300, and Zn600 nanocomposites are termed as Zn100F, Zn300F, and Zn600F, respectively.

2.6. UV resistance of coated fabrics

The UV transmission spectra (Lambda 35; Perkin Elmer, USA) of all ZnO nanoparticles were measured with the wavelength ranging from 280 to 400 nm.The ASTM D6603 standard was used to obtain the UVprotection factor (UPF) for all nanocomposite coated cotton fabrics using the following relation [42]:

$$UPF = \frac{\sum_{290}^{400} E(\lambda) \times S(\lambda) \times \Delta\lambda}{\sum_{290}^{400} E(\lambda) \times S(\lambda) \times T(\lambda) \times \Delta\lambda} \quad (1)$$

where $S(\lambda)$ is the solar spectral irradiance (W^{-2-1}), $E(\lambda)$ the relative erythemal spectral effectiveness, $T(\lambda)$ the spectral trans- mittance, and $\Delta(\lambda)$ the wavelength interval.

Table 1
The crystal size, miller indices and d-spacing value of ZnO nanoparticles at three different calcination temperatures.

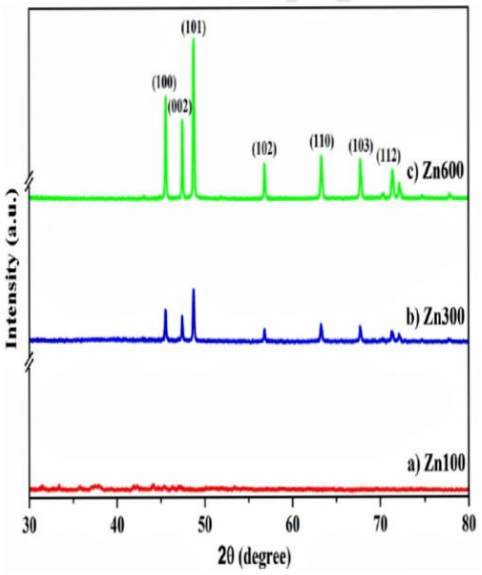

Fig. 2. XRD spectra of ZnO nanoparticles calcined at different temperatures.

Table 1
The crystal size, miller indices and *d*-spacing value of ZnO nanoparticles at three different calcination temperatures.

Temperature	Average crystallite size (nm)	Miller indices (*hkl*)	FWHM (2θ)	*d*-Spacing (Å)
Zn100	-	-	-	-
Zn300	39.34	(1 0 0)	0.1968	1.4648
		(0 0 2)	0.1476	1.3640
		(1 0 1)	0.1968	1.3039
		(1 0 2)	0.1968	1.0453
		(1 1 0)	0.2952	0.9239
		(1 0 3)	0.2460	0.8667
		(1 1 2)	0.2460	0.8322
Zn600	43.63	(1 0 0)	0.1968	1.4617
		(0 0 2)	0.1968	1.3613
		(1 0 1)	0.1968	1.3017
		(1 0 2)	0.2952	1.0438
		(1 1 0)	0.2952	0.9231
		(1 0 3)	0.2460	0.8661
		(1 1 2)	0.2460	0.8316

2.7. Antimicrobial studies

2.7.1. Collection of microorganisms and culture

The bacterial cultures, namely gram-positive Staphylococcus aureus (S. aureus: ATCC 6538P) and gram-negative Escherichiacoli (E. coli: ATCC 9677), were obtained from the National Collection of Industrial Microorganisms (NCIM), National Chemical Laboratory, Pune, India. The sterile AATCC Mueller Hinton Agar (M391;HiMedia, India) was prepared and plated. Fresh bacterial inoculums were prepared by inoculating a loopful of test organisms into nutrient broth and then, incubated at 37 ºC for 5–8 h till a moderate turbidity was developed. A loop of culture was swabbed onto the Mueller Hinton Agar for testing the antimicrobial activity of all ZnO nanoparticles and its coated fabrics by agar well diffusion and disk diffusion methods respectively.

2.7.2. Agar well diffusion method

The qualitative antibacterial assessment was performed against E. coli and S. aureus by agar well diffusion method [43]. A fine agar well was made in the inoculated agar medium using a sterile cork borer. The diameter of each well of the bacteria-inoculated agar plates was kept constant as 7 mm. A concentration of 100 mg of three ZnO nanoparticles was added in the wells of three separate agar plates. Then, the inoculated plates were incubated at 37ºC for approximately 24 h, subsequent to that the diameter of zone of inhibition was measured by millimeter ruler.

2.7.3. Agar disk diffusion method

The disk diffusion method was used to explore the qualitative antibacterial assessment of un-coated (UC-CF) and ZnO nanocomposite coated cotton fabrics (Zn100F, Zn300F, andZn600F) against pathogenic bacteria namely E. coli and S. aureus.The UC-CF and ZnO nanocomposite-coated fabrics were cut intoa circular sample of 10 mm diameter [33,44]. The obtained samples

were aseptically pressed on the agar surface. The inoculated plates were incubated at 37ºC for 18–24 h.

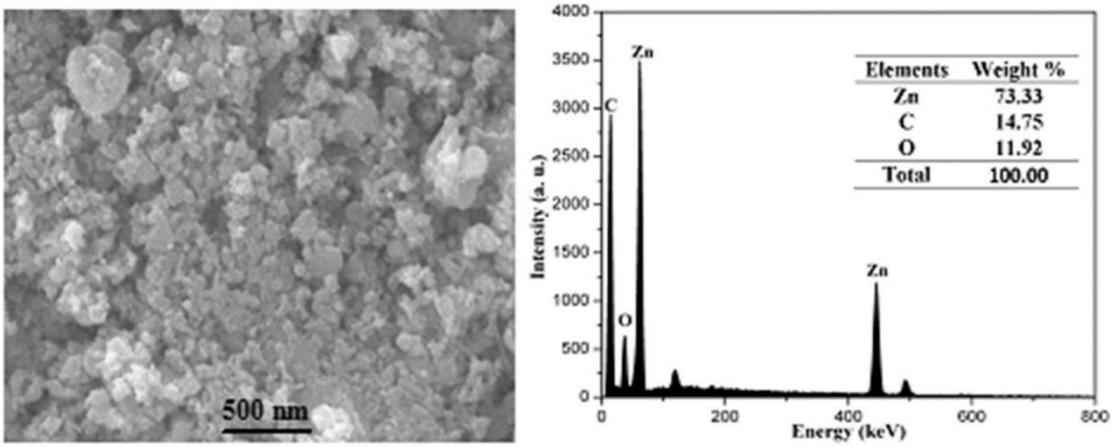

a) SEM image b) EDX spectra

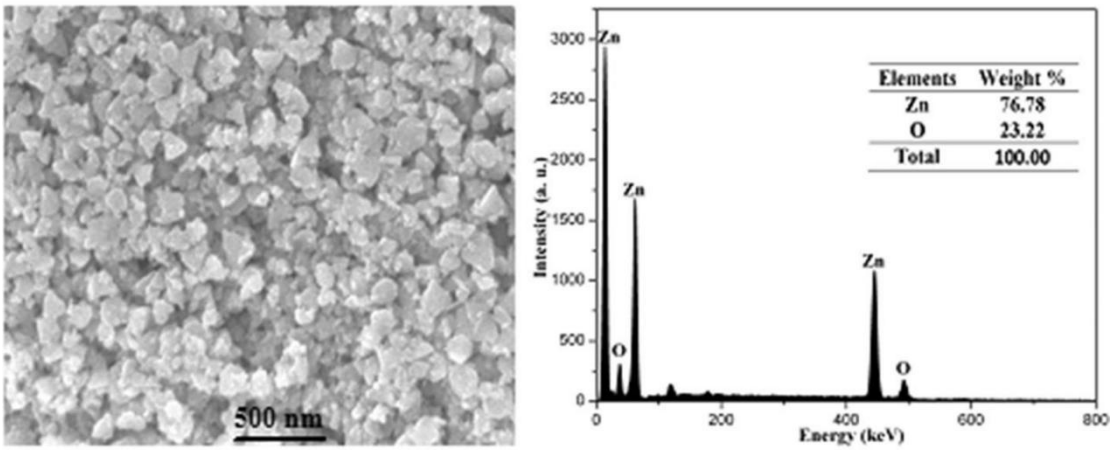

c) SEM image d) EDX spectra

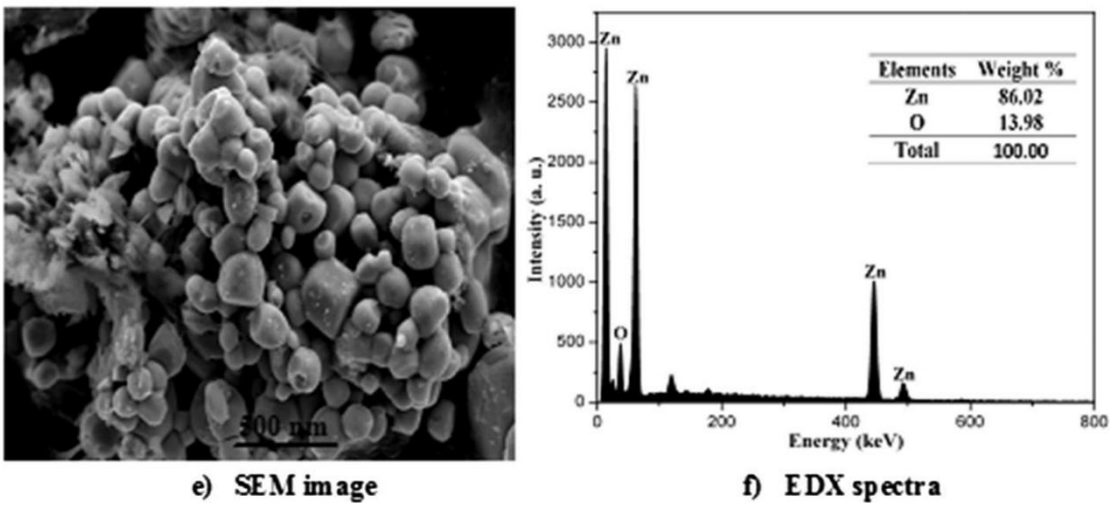

e) SEM image f) EDX spectra

....

2.7.4. Wash durability of coated fabrics

The IS: 687-1979 standard was followed to determine the wash durability of the ZnO nanocomposite coated cotton fabrics(Zn100F, Zn300F, and Zn600F). This test was carried out using a neutral soap solution at 40 ± 2ºC for 30 min. After drying, the test fabrics and the control were assessed for antimicrobial activity using the AATCC 100 procedure up to 10 laundry cycles (i.e., 10 industrial washes: 1 industry wash is equal to 15 home washes).

2.7.5. Percentage reduction test

The percentage reduction assessment was performed in both un-coated and ZnO nanocomposite-coated cotton fabrics. The nanocomposite coated cotton fabrics were first dipped separately into inoculated bacterial culture, that is, in both E. coli and S. aureus. Then, the dipped cotton fabrics were incubated at 37ºC for 18–24 h [45]. The incubated culture (0.1 mL) was pipetted and then, spread on the sterile agar plate. These plates were again incubated at 37 ºC for 24 h. The percentage of bacterial reduction was calculated employing the viable cell count method, using the following relation [42]:

% Bacterial Reduction=[(퐴 − 퐵)/퐴] × 100

where A is the initial number of cells and B the final number of cellscotton woven fabric (116 ends per inch and 84 picks per inch) using pad-dry-cure method [41]. The size and mass of the cotton fabric used in the present study were30×30 cm and 138.84 g $^{-2}$respectively. The coated cotton fabric was dried at 80ºC for 20 min. The un-coated

.

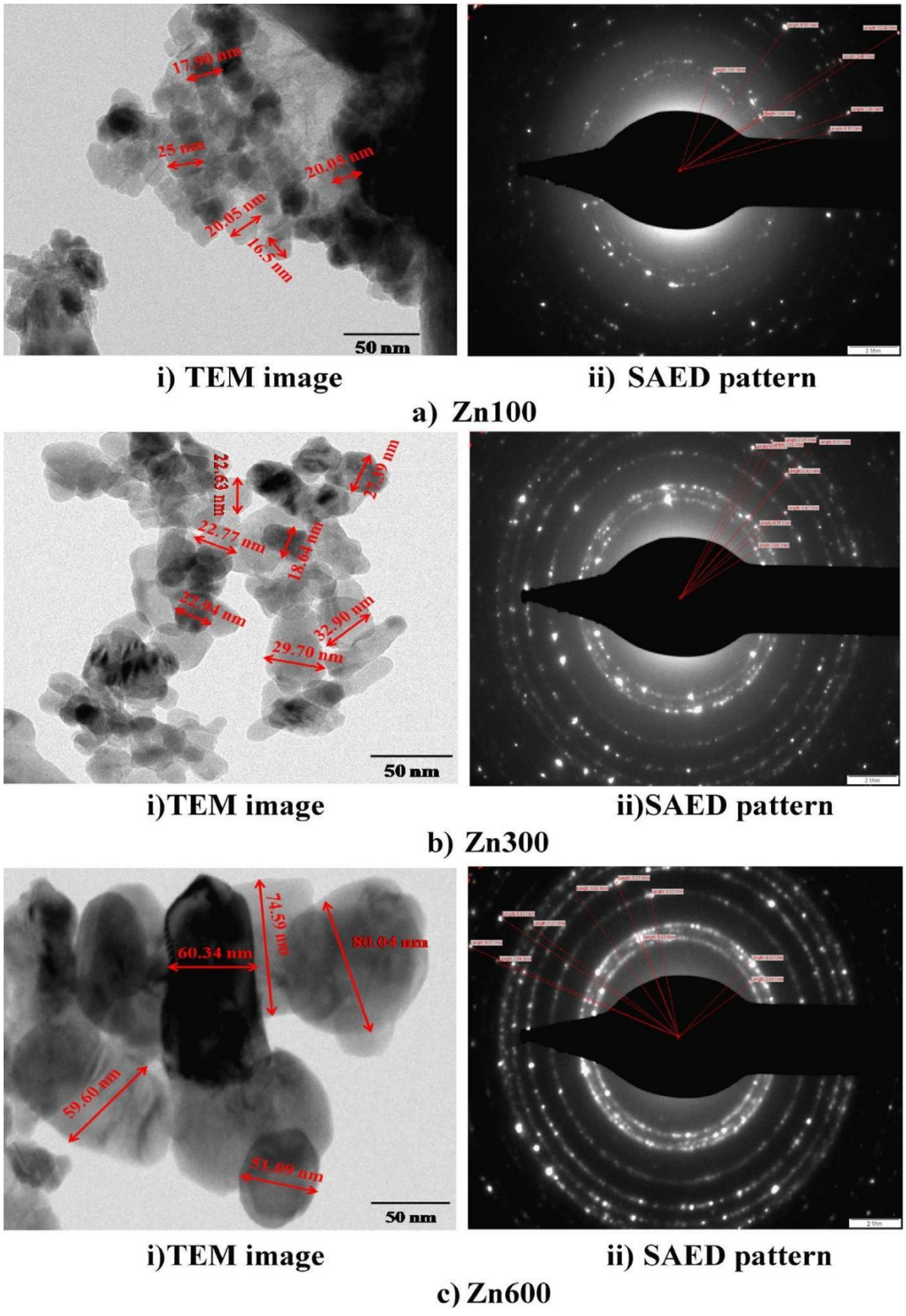

Fig. 4. TEM images and SAED pattern of ZnO nanoparticles calcined at different temperatures.

Result and discussion.

ZnO NPs Synthesis and its Characterization

Effective ZnO NPs is synthesized successfully using the leaf extract of C. verrucosa because of their exclusive phytochemicals and metabolite abundance. Presence of sunlight was also helpful for successful and effrective green synthesis of ZnONPs. The phyto-moleculespresent in C. Verrucosa extract are generally photosensitive flavoproteins and thus they enhance the reduction of metal ions for the e_ective synthesis and capping of NPs [51,52]. The color of the solution was turned from pale yellow to white, confirming ZnO NPs synthesis [46]. The synthesized ZnO NPs were reported to form white precipitate using plant extracts of di_erent species like Rutagra veolens [53]n and Plectranthus amboinicus [54], among others, which is in accordance with the results of our research. This visual color is the preliminary indication of NPs synthesis. The UV visible absorption spectrum was performed to validate the biosynthesized NPs at the initial stage and evaluated in the range of 300–600 nm as shown in Figure 2a. The distinct peak of 375 nm is unique to ZnO nanoparticle formation due to their high excitation binding energy [55]
confirming that leaf extract act as reducing agents during NPs formation. Bandgap increases with the decrease in particle size because of which blue shifting occurs in ZnO NPs compared to bulk ZnO [56].

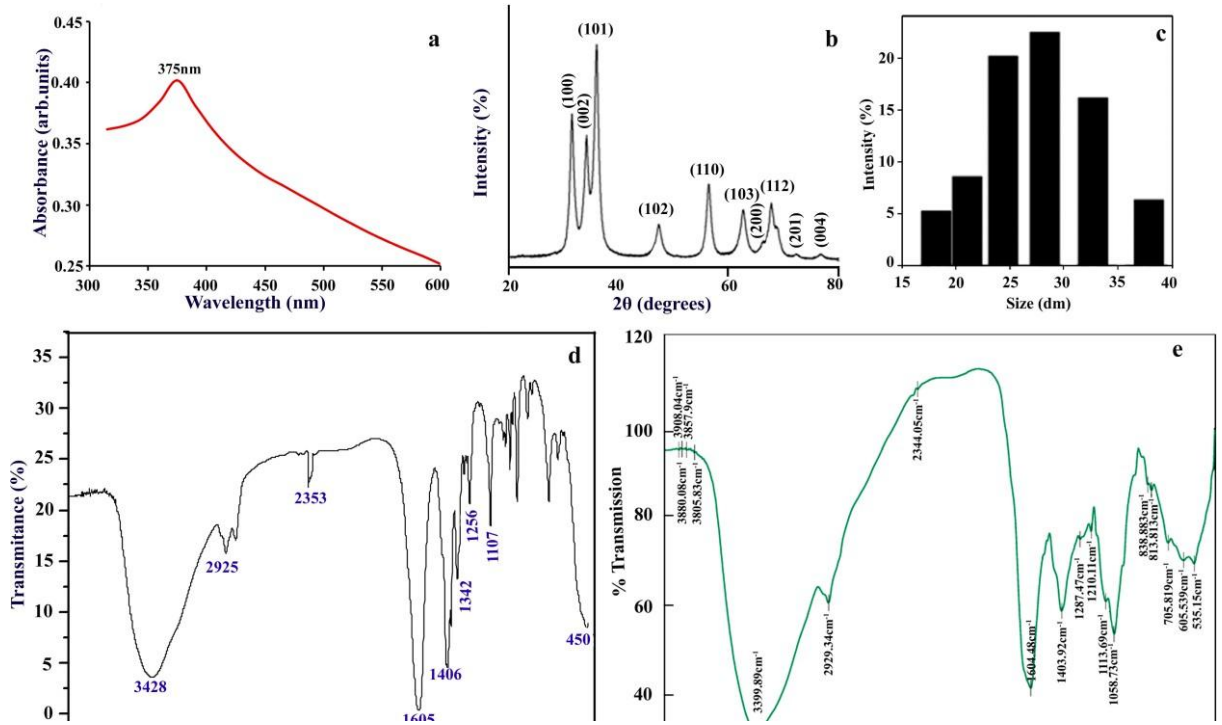

Figure 2. Characterization of green synthesized ZnO nanoparticles using *C. verrucosa* leaf. (**a**) UV-visible spectroscopy, (**b**) XRD, (**c**) Histogram showing DLS pattern of size distribution of ZnO-NPs, FTIR spectrum of (**d**) ZnO NPs and (**e**) leaf extract of *Crotalaria.*

The synthesized ZnO NPs have undergone X-ray diffraction to achieve crystallinity and to calculate average particle size. X-Ray Diffraction patterns of the biosynthesized ZnO NPs are presented in Figure 2b. XRD spectral analysis displays number of strong diffraction peaks corresponding to Bragg reflections with 2Θ values of 31.94º, 34.28º, 36.20º, 47.49º, 56.54º, 62.86º, 66.43º, 67.89º and 68.99º, that are indexed to (1 0 0), (0 0 2), (1 0 1), (1 0 2), (1 10), (1 0 3), (2 0 0), (1 1 2), and (2 0 1) planes respectively. This can be attributed to ZnO hexagonal wurtzite phase structures as per Joint Committee on Powder Di_raction Studies Standards (JCPDS file number: 36-1451) [57] and this confirms the crystalline structure of ZnO NPs. The crystallite size of ZnO NPs with the assistance of the highest peak
by the Debye–Scherrer equation [58] obtained was calculated out to be 17.47 nm from a high-intensity peak. The broadening of a peak in a diffraction pattern suggests that the particles of the prepared NPs are in the nanometer range.

DLS is mainly used to measure the hydrodynamic diameter depending on particle Brownian movement of nanoparticle in suspension and the average hydrodynamic diameter measured by DLS histogram is 27 nm (Figure 2c) which varies from the size assessed from TEM and XRD. This difference in measured NP size with polydispersity index (pdi) value of 0.488 is attributed to the polydisperse nature of nanoparticles indicating non-uniform distribution of particles in nanosuspension and its occurrence in the form of aggregates which is evident from TEM images. Substance-specific vibrations of the molecules contribute to the specific signals obtained by infrared spectroscopy. Spectroscopy of FTIR is a non-invasive and effective technique for investigating the role of functional atoms or biomolecules present in leaf extract which helps in the reduction and stabilization of NPs, also analyzes chemical bonds of NPs by its absorbance and transmittance value in the range of 400 to 4000 cm-1. FTIR spectrum of the biosynthesized ZnO NPs and aqueous leaf extract of C. verrucosa are illustrated in Figure 2d,e respectively, showing the broad peak at 3428 cm-1 for biogenic ZnO-NPs and 3399.89 cm-1 for leaf extract, which correspond to H bonded O–H stretching vibrations of polyphenols, alcohols [59,60]. FTIR spectral band exhibits weak absorption near 2925 and 2353 cm-1 (in case of ZnO NPs) and 2929.34 and 2344.05 cm-1 (for leaf extract), are attributed to C–H stretching vibration which depicts the presence of alkanes group. The peak at 1406 cm-1 (for ZnO NPs)and 1403.92 cm-1 (for leaf extract) refers to C-N vibration stretch in protein amide linkages [61,62].

The sharp absorption peak observed at 1603 cm-1 for ZnO and 1604.48 cm-1 for leaf extract areassigned to the N–H bending vibration of amine or amide groups [63]. The band observed at 1107 cm-1(for ZnO NPs) and 1113.69 cm-1 (leaf extract) are assigned to C–O stretching alkoxy group or C-O-H in secondary and tertiary alcohols [64]. FTIR spectrum wavenumber of ZnO NPs (Figure 2d) confirms the presence of polyphenol, flavonoids, carbonyl, and aliphatic amine group of the plant extract are
documented to act as both reducing and capping [65]. A sharp peak in the lower energy region was found at 450 cm-1 confirming Zn–O bond bending vibration as metal-oxygen are reported in the range of 400 to 600 nm [66]. Therefore, FTIR assessed for C. verrucosa mediated ZnO NPs (Figure 2d) corroborates with the result of FTIR spectrum of leaf extract, which shows that the organic compounds
(phenols and flavonoid) of C. verrucosa still retain their original properties after calcination during ZnO synthesis and hence reduced the synthesized ZnO NPs.

The TEM images of ZnO NPs at 200 nm (Figure 3a), 100 nm (Figure 3b) and 50 nm (Figure 3c,d) are shown. The TEM is a powerful tool for characterizing the ZnO NPs and was performed to understand the morphology and size of the NPs. TEM image of ZnO NPs shows a slight intense capping on the periphery of the nanoparticle surface due to biomolecules of aqueous leaf extracts showing that it acts

as a reduction and capping agent. TEM confirms that NPs present in slightly aggregates form and show the size range of 16–38 nm particle sizes and the average particle size found out to be 27 nm and hexagonal shape (Figure3.)

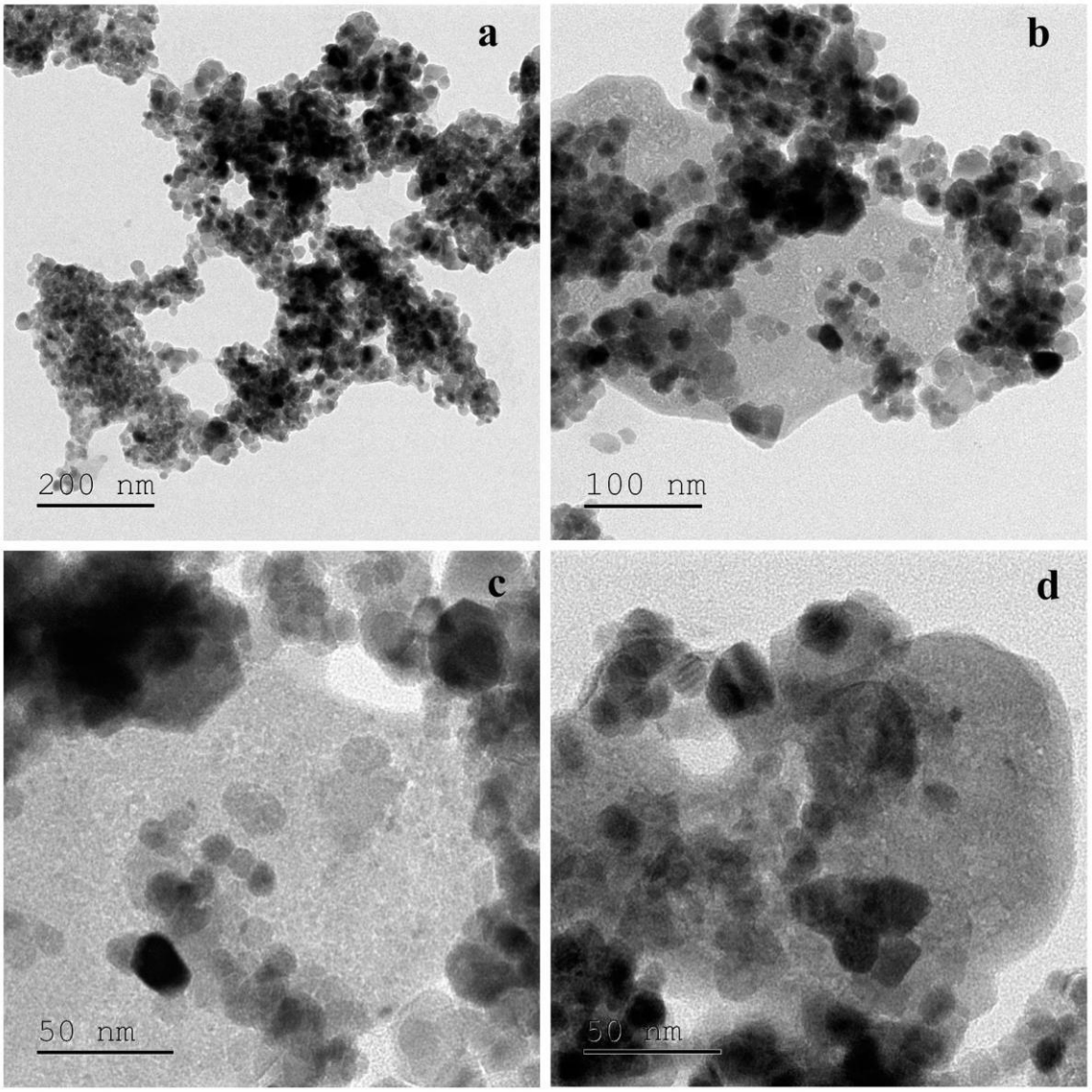

Figure 3. TEM image of nano-ZnO particles using *C. verrucosa* leaf extract at different scale: (**a**) 200
nm, (**b**) 100 nm, (**c**,**d**) 50nm.

Zeta potential povides the zeta value which shows surface charge and stability of ZnO NPs (prepared using C. verrucosa leaf extract) was -21 mV (Figure 4a) demonstrating its stability. The hydroxyl group of C. verrucosa leaf extract is responsible for reduction of metal ion due to its strong binding a_nity so that they can act as capping agent to avoid nanoparticle aggregation assuring its negative charge [38] and are in agreement with biosynthesized ZnO NPs from S. album leaf extract [67] and using C. halicacabum leaf extract [66]. TGA is used to assess the thermal stability of the synthesized NPs (20 mg) by subjecting the NPs to a temperature range of 0–1000 ℃ (Figure 4b)
The reduction in weight measured at ~120 ℃ corresponds to the desertion of humidity. The actual reduction of weight was observed between ~340 and 550 ℃, which corresponds to the

elimination and decay of the very minute amount of organic compounds present in the sample during the green synthesis and decay of Zn and oxygen were measured at ~800 -C [68]

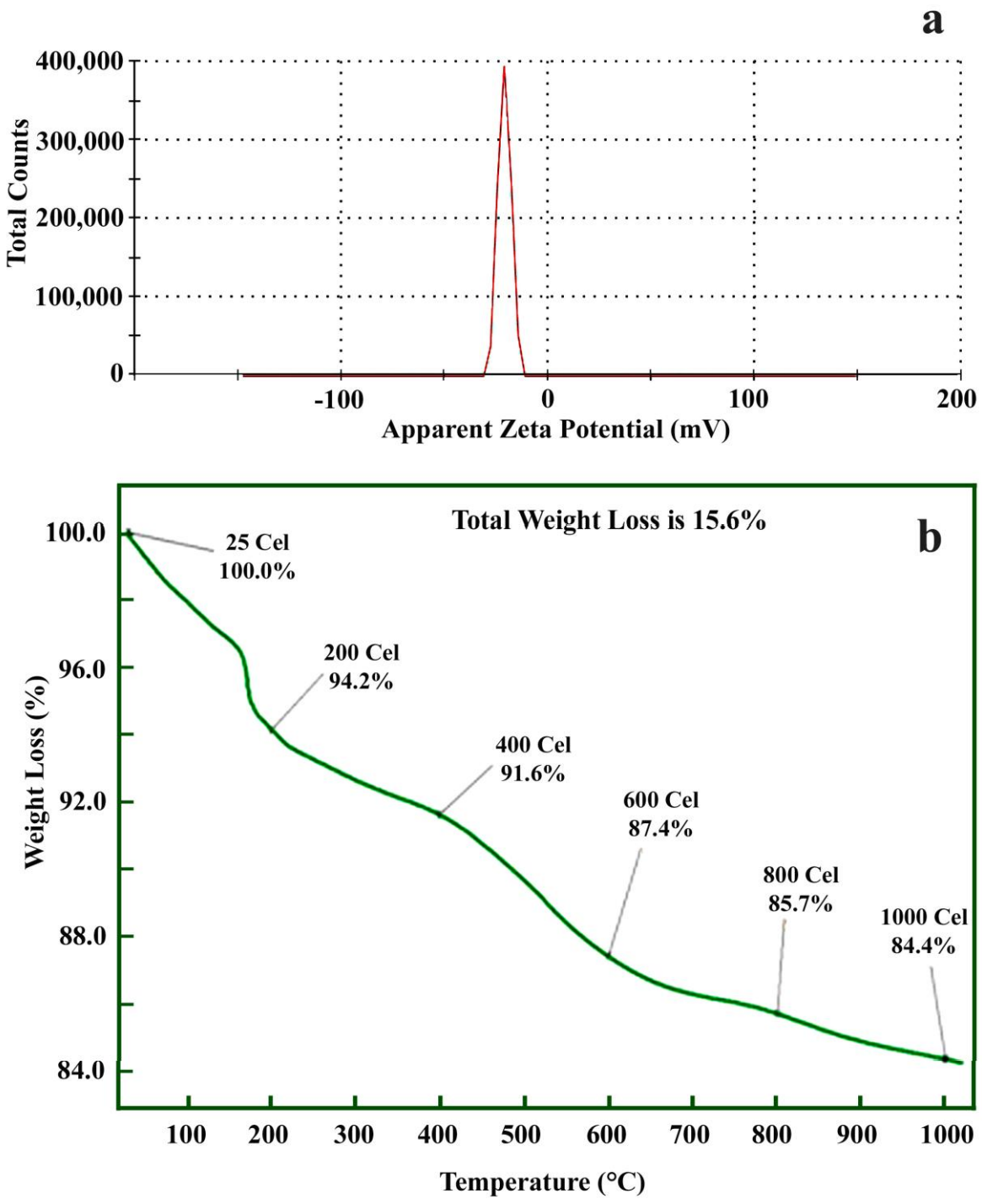

Figure 4. (**a**) Zeta potential analysis and (**b**) TGA analysis of green synthesized nano ZnO particles using C. verrucosa leaf extract.

The XRD pattern of the calcined samples at three different temperatures is shown in Fig. 2. The analysis of the structure and sizedetermination of ZnO nanocrystals are carried out using the following modified Scherrer equation [46]:

=

where β is defined as β= (^{2}observed -^{2} instrumental) $^{1/2}$ K is the shape factor equals to 0.89, k the X-ray wave length for Cu k radiation (k = 1.5418 Å), h the Bragg diffraction angle (in degrees)292 and b the full-width at half-maximum (FWHM) of the observed peak. Fig. 2a shows the XRD pattern of the low temperature calcined sample. There are no peaks in the diffractogram of sample calcined at 100 ºCdue to amorphous nature of the prepared ZnO particles.Fig. 2b and c reveal similar 2h value with different intensities due to the increase in calcination temperature.The diffraction peak pattern of Zn300 observed at 2h = 31.7,34.4, 36.2, 47.5, 56.5, 62.7, and 67.8º and the Zn600 peaks at 2h= 31.8, 34.4, 36.3, 47.6, 56.6, 62.8, and 67.9º respectively, correspond to the planes (1 0 0), (0 0 2), (1 0 1), (1 0 2), (1 1 0), (1 0 3),and (1 1 2). These results confirm the hexagonal structure of the prepared ZnO nanoparticles (JCPDS file no. 076-0704) [21]. The intensity of the mentioned peaks increases with increasing calcination temperature up to 300 ºC. The crystallite sizes of ZnO nanoparticles are found to be 39.34 and 43.63 nm respectively for Zn300 and Zn600. The correlation of XRD peak intensity with a calcinations temperature observed in our study is in line with the observation made on ZnO nanoparticles prepared at different calcination temperatures [47].

Heat treatment under 200 ºC can only eliminate residual water while the other organic components still exist. The absence of peak in the XRD pattern in Zn100 indicates the amorphous nature.

When the sample is calcined at 100 ºC (Zn100), the residues of organic impurities are known to exist and hence, it suppresses the formation of crystals. On the other hand, the observed decrease in the width of crystal peak with an enhancement in calcination temperature is ascribed to the growth of crystals and construction of larger clusters. The increase in crystallite size due to an increase in calcination temperature is shown in Table 1.

Effect of ZnO nanoparticles calcined at different temperatures on their structure and morphology is studied using SEM (Fig. 3)and TEM (Fig. 4) observations.

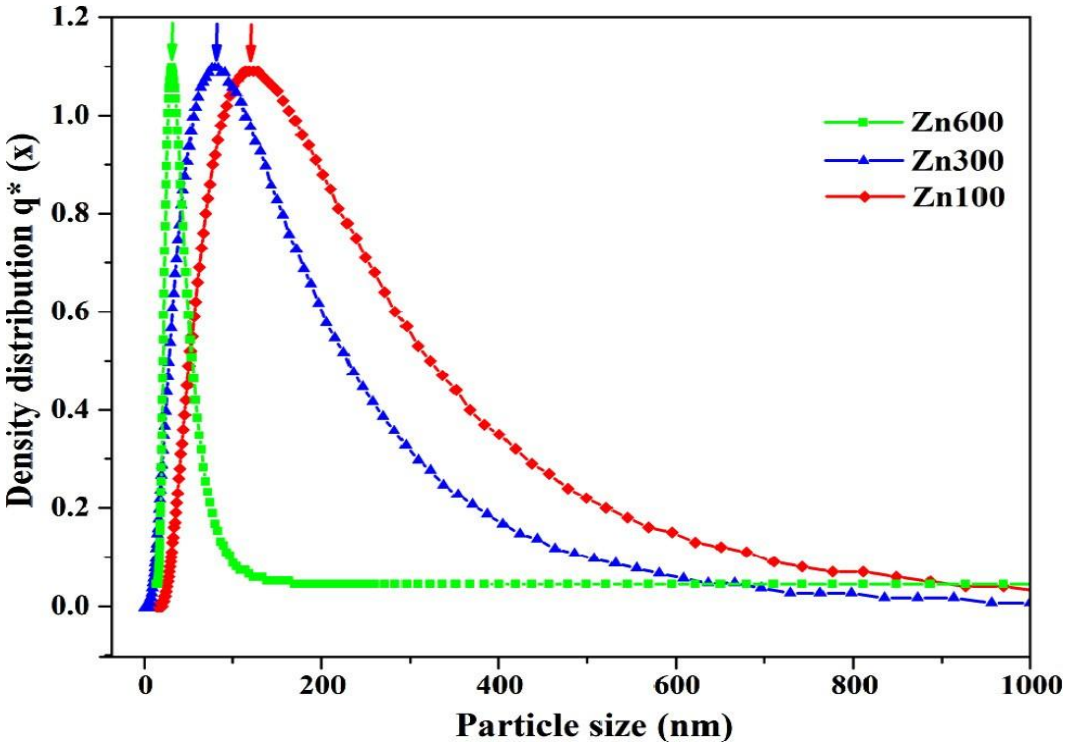

Fig. 5. Particle size distribution curve of ZnO nanoparticles

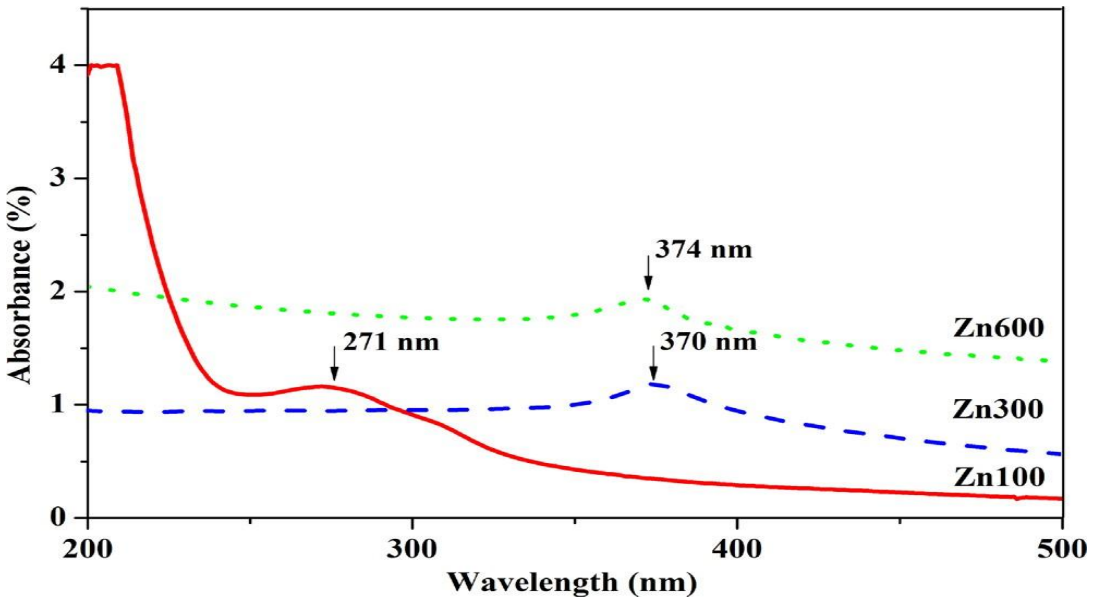

.Fig. 6. UV–visible spectrum of ZnO nanoparticles calcined at different temperature.

Table 2
Particle size and BET surface area analysis for ZnO nanoparticles.

Synthesis methods	Particle size (nm)	BET Surface Area ($m^2 g^{-1}$)
Zn100	107	112.8
Zn300	81	227.5
Zn600	20	359.3

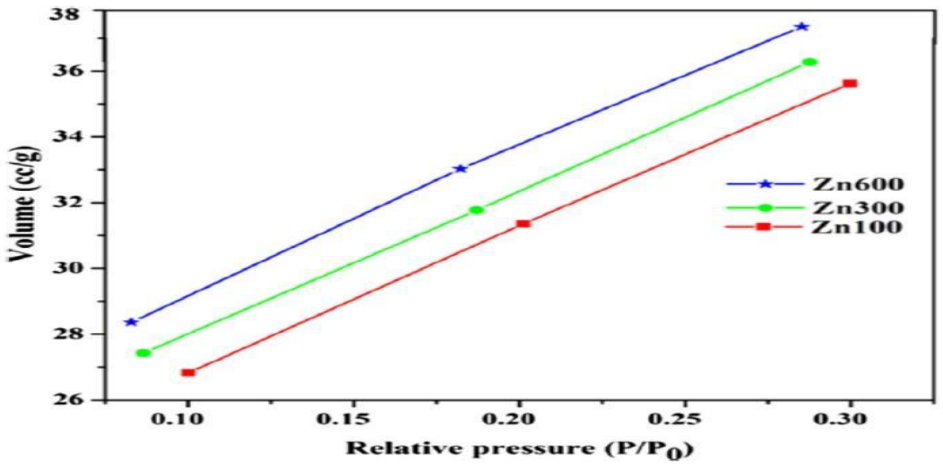

Fig. 7. BET plot for surface area of ZnO nanoparticles.

The morphological changes occurred in Zn600 nanoparticles are totally different from occurred in Zn100 and Zn300. Zn600 shows spherical morphology,whereas Zn100 and Zn300 nanoparticles appear in irregular shape with an aggregated morphology.The average particle size of the ZnO nanoparticles observed through TEM images is 19.9, 53.39, and 65.13 nm respectively for the Zn100, Zn300, and Zn600 nanoparticles. The selected area electron diffraction (SAED) pattern (Fig. 4) of ZnO nanoparticles depicts concentric diffraction rings confirming the crystallinity of Zn600 nanoparticles than Zn100 and Zn300 nanoparticles. Thus, high temperature calcination of ZnO nanoparticles enhances their crystallinity upon heat treatment from 300 to 600 ºC. This is line with the earlier observation that higher calcination temperature (above600 ℃) enhances the crystallization of the metal oxides by decreasing the defects in crystals [46].

Fig. 5 shows that the average particle size for Zn100, Zn300, and Zn600 nanoparticles is 107, 81, and 20 nm respectively. Thus, the above observation reveals the influence of calcination temperature on the reduction of particle size. However, ZnO nanoparticles synthesized from this investigation are highly stable due its structure and morphology formed during the green synthesis. UV–vis spectra of Zn100, Zn300 and Zn600 nanoparticles given in Fig. 6 reveal absorption peaks at 271, 370, and 374 nm respec -tively. The observed peak at 271 nm for Zn100 nanoparticles may be due to the presence of impurities in plant extract. This means that an increase in the calcination temperature leads to an increase in the absorbance of ZnO nanoparticles by decreasing the particlesize [48]. The calcination temperature influences the control of particle size, which supports the results observed in our study [49]. To investigate the effect of different calcination temperatures on the specific surface area of ZnO nanoparticles, BET surface area analysis is carried out. The specific surface area of ZnO samples are given in Table 2 and Fig. 7. The obtained specific surface area of Zn600 is quite higher (359.3 m2 g -1) than that of Zn100 andZn300 (112.8 and 227.5 m2 g -1, respectively).It is revealed from the above observation that the ZnO nanoparticles processed at three different calcination temperatures influences the surface area. It is also evident that higher calcination temperature enhances the formation of specific surface area and reactivity due to the formation

of dense corner size andstructural defects [50.

Table 3
Contact angle measurement and UPF value of ZnO nanocomposites coated and un-coated fabric samples.

Sample	Contact angle (°)	UPF
Before wash		
UC-CF	0	13.9
Zn100F	101 ± 2	40.9
Zn300F	125 ± 1	60.6
Zn600F	155 ± 3	87.8
5th Wash		
Zn100F	96 ± 4	31.3
Zn300F	117 ± 2	57.8
Zn600F	136 ± 1	67.1
10th Wash		
Zn100F	91 ± 1	23.7
Zn300F	102 ± 2	48.8
Zn600F	127 ± 4	56.4

The SEM images of synthesized ZnO nanoparticles coated on cotton fabrics are shown in Fig. 8. It is observed that Zn600 coated cotton fabric (Zn600F) has a higher adsorption on the cotton fabric surface than Zn100 and Zn300 coated cotton fabrics (Zn100F and Zn300F). As seen from the SEM image, ZnO nanocomposite coated cotton fabric shows high-quality distribution of the nanocomposite over the fabric than that of the coated fabric using other process methods, as reported in our earlier studies [51,52]. The UV-protection studies on ZnO nanocomposite-coated and un-coated fabrics are shown in Table 3.

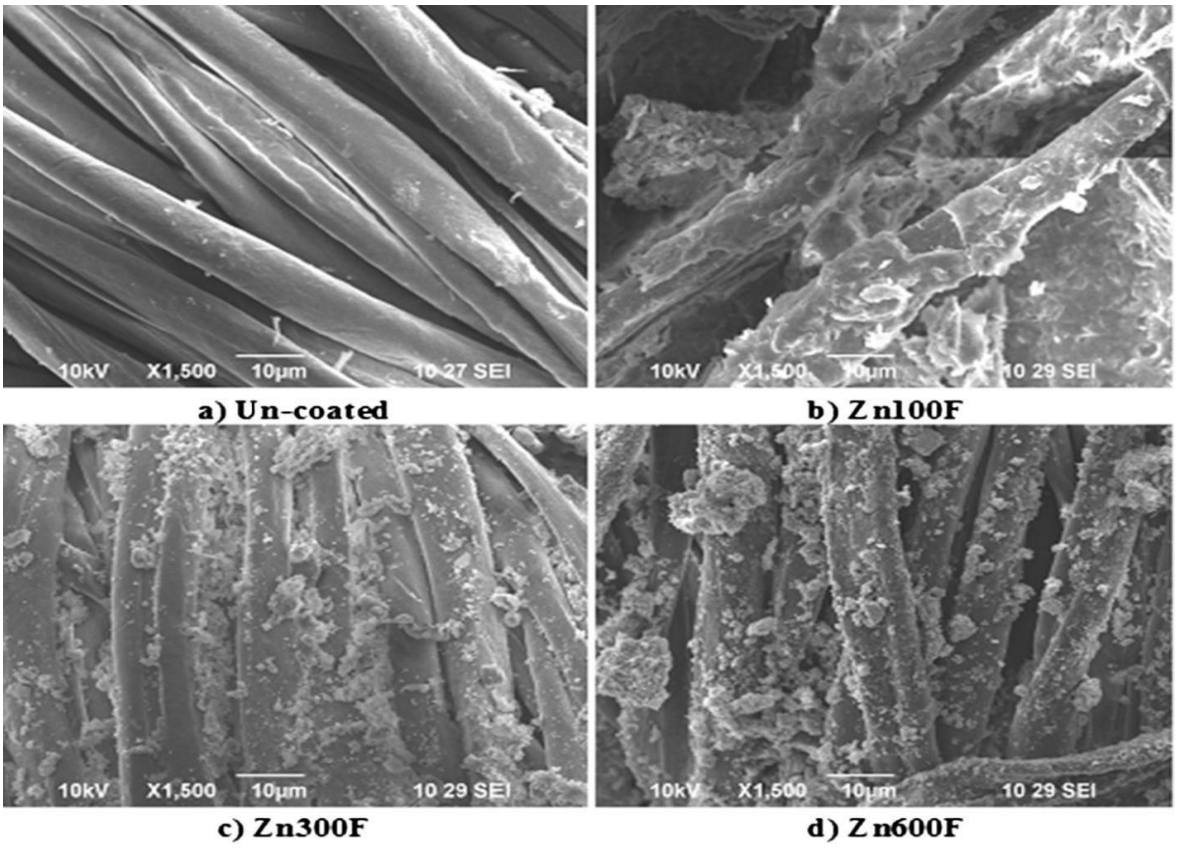

Fig. 8. SEM images of un-coated and ZnO nanoparticles coated fabrics

The ZnO nanocomposite coated fabrics block both UV-A and UV-B radiations. The hightemperature
calcination of ZnO nanocomposite exhibits much protection to UV-B than low-temperature calcination. These results confirm the effect of high-calcined ZnO nanoparticles with high optical polarization and surface area [53]. On the basis of ASTM D6603 standard data (UPF: >50 has high UV protection), the calculated UPF value is found to be 87.8 for Zn600F whereas the UPF for Zn100F and Zn300F is 40.9 and 60.6 respectively. The above results correlate and confirm the previous observation that the higher calcination of ZnO nanoparticles enables better UV-protection because of better nucleation of particles during high temperature treatment towards nanoscale [1]. The ZnO nanoparticles green-synthesized from A. indica shows higher UPF than other chemically synthesized particles. The enhanced UV-protection offered by the fabrics coated with nanocomposite is attributed to the observed difference in the structural purity and morphology [54,55].

3.1. Antimicrobial assessment of ZnO nanocomposite-coated fabrics

The zone of inhibition observed in Zn100, Zn300, and Zn600 nanocomposite-coated fabrics is shown in Fig. 9. The well-loaded with Zn600 nanoparticles show the maximum zone of inhibition

- against E. coli and S. aureus at a concentration of 100 mg ml -1
- (22.89 ± 0.06 and 24.62 ± 0.08 mm). In contrast, Zn100 and Zn300 nanoparticles respectively show lesser inhibition zone against E. coli (19 ± 0.07 and 20.1 ± 0.05 mm) and S. aureus (20.1 ± 0.04 and 21.2 ± 0.07 mm). The above assessment shows an increase inthe antibacterial activity with an increase in calcination temperature, which is ascribed to the fact that the increasing calcination temperature results in a reductionnof size, thereby enhancing the reactive surface of the particles leads to higher

antimicrobial property. Hence, the degree of contact with bacteria is increased withthe addition of smaller particles with high surface area, which results in the formation of a wide zone of inhibition [49,56].

The screening of the antibacterial activity for un-coated and Zn100F, Zn300F, and Zn600F nanocomposite-coated cotton fabrics is assessed bymeasuring the zone of inhibition, asshown in Fig.10.

According to the size and surface area of particles, Zn600F yields better inhibitory action against E. coli (25.13 ± 0.05 mm) and S. aureus (30.17 ± 0.03 mm) when compared to Zn100F and Zn300F

coated fabrics. Thus, the observed antibacterial action of the green synthesized

ZnO is higher than that of the conventional ZnO nanocomposite coated cotton fabrics against E. coli (22 mm) and S. aureus (25 mm) [55,57]. In case of un-coated fabrics, there is no evidencerecorded for the formation of inhibition zone. The above bacterial susceptibility investigations on ZnO nanoparticles synthesized using plant extract confers their exotic medicinal properties and therapeutic uses.

3.2. Percentage reduction test

The quantitative evaluation of the antibacterial activity for the un-coated and ZnO nanocomposite-coated cotton fabrics carried out by percentage reduction test is summarized in Table 4.

Table 4
Bacterial reduction percentage of ZnO nanocomposites coated fabrics.

No. of washes	Bacterial reduction percentage (%) for the coated fabrics					
	Zn100F		Zn300F		Zn600F	
	E. coli	*S. aureus*	*E. coli*	*S. aureus*	*E. coli*	*S. aureus*
0 wash	68 ± 0.13	75 ± 0.21	87 ± 0.17	92 ± 0.33	96 ± 0.10	98 ± 0.24
5th wash	63 ± 0.12	68 ± 0.51	79 ± 0.37	80 ± 0.29	85 ± 0.61	87 ± 0.38
10th wash	32 ± 0.08	41 ± 0.01	45 ± 0.22	47 ± 0.61	48 ± 0.23	49 ± 0.02

The results show that Zn600F fabrics has higher bacterial reduction percentage in both E. coli andS. aureus (96% and 99%) than Zn100F (68% and 75%) and Zn300F (87% and 92%) fabrics, whereas un-coated cotton fabrics has no bactericidal activity.After 5th and 10th washes, the bacterial growth is decreased owing to the removal of ZnO nanocomposite from the cotton fabric surface [49]. A similar observation is made in our previous investigation on the cotton fabrics coated with herbal nanoparticles where in consequent washes led to the removal of nanoparticles from fabrics, resulting in a decrease in antimicrobial activity [58]. Wash durability of the nanocomposite-coated cotton fabrics shows higher wash durability than that of the fabrics reported in previous studies[59,60]. It might be due to high stability and high distribution on the cotton fabrics.

3.3. Water repellant property

Sessile drop method is used to analyze the surface contact angle to get a comparative assessment of the coated fabric (Zn100F, Zn300F, and Zn600F) and un-coated fabric in view of its water repellent property. Interestingly, high degree of hydrophilic property is noticed for the un-coated fabric due to the presence of higher hydroxyl groups on its surface. As soon as the water droplet is placed on the cotton fabric, it gets absorbed easily on the surface of the un-coated fabric (Fig.11).

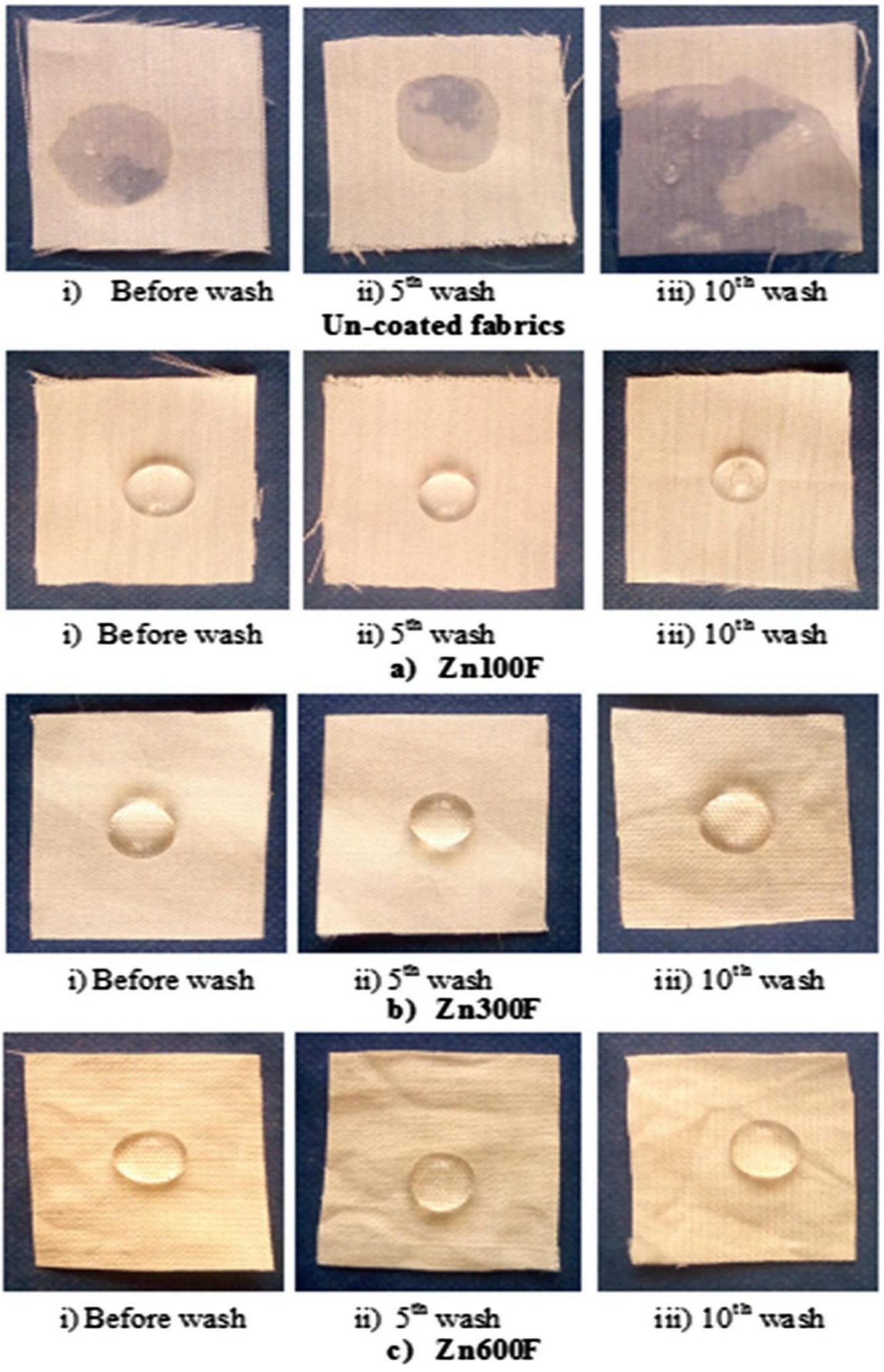

Fig. 11. Water repellant property of un-coated and coated fabrics surface.

In contrast, fabrics coated with ZnO nanocomposite show enhanced hydrophobicity, especially ZnO calcined at 600 ºC (155 ± 3_). The observed higher hydrophobicity of the ZnO nanocomposite-coated fabric is a due to lower surface energy and the well-bound layer formation of the ZnO nanoparticles over the fabric, causing a net reduction in fabric pore sizes. It is seen that the fabrics coated with ZnO nanoparticles processed at low temperature calcination (Zn100 and Zn300) show different contact angle values (i.e., 101 ± 2_ and 125 ± 1_ respectively), as shown in Table 3.

The change in the morphology of the ZnO nanoparticles-coated fabrics plays a major role in inducing the change in water-repellent property, as supported by other researchers [61,62]. Even after subsequent (5th and 10th) washes, the fabric surface shows hydrophobic nature (Table 3). From aforementioned investigation, it is evident that the fabric coated with ZnO nanocomposite has higher hydrophobic nature as well as higher retention of water-repellent property than un-coated fabric. It is also an interesting phenomenon that smaller particle size with high surface area improves hydrophobicity of ZnO nanoparticles-coated fabrics,favoring the self-cleaning applications of green-synthesized ZnO nanoparticles. The increased hydrophobicity is also attributed to the changes in the surface morphology of textile fibers and its surface energy emerging out of nanocomposite coated on the fabrics[17,63].By reviewing all the studies, it is found that ZnO nanoparticles calcined at 600 ºC show good antibacterial, UV -resistant, wash durability, and water-repellent properties. These observations favor the application of such green-synthesized ZnO nanoparticles as an effective nanomaterial for textile-processing technology to be used in medical textiles.

4. Conclusion

The ZnO nanoparticles were green-synthesized from A. indica without adding any chemical additives. High temperature calcination of the prepared ZnO nanoparticles considerably influenced the formation of favorable crystal structure, particle size, and morphology with specific surface area. It is also found that the fabrics coated with ZnO nanocomposite obtained by calcination at 600 ºC show maximum zone of inhibition against E. coli (25.13 ± 0.05 mm) and S. aureus (30.17 ± 0.03 mm), higher UV-protection (87.8UPF), and water-repellent property with enhanced wash durability than those coated with particles calcined at 100 and 300 ºC. Hence, it is concluded that optimizing the green synthesis of ZnO nanoparticles by varying calcination temperature renders an effective strategy to produce favorable nano-metal oxides with interestingbiological properties for biomedical and textile applications.

C. verrucosa is reported to show cytotoxic and anticancer activity and the ZnO NPs synthesized using its leaf extract was found to be more effective than sole leaf extract treatment. Nanosized ZnO of size 16–38 nm was synthesized biologically using C. verrucosa leaf extract and was characterized to determine its unique properties that consequently displayed potent antibacterial activity against the studied MDR human pathogenic bacteria. Further, cytotoxicity assay and its visualization results revealed it as a selective substitute for cancer therapy specifically against cervical and prostate cancer with its selective targeting property within the cell. However, there is a need to explain further the exact mechanism of inhibitory action in microbes and the studied cancer cells due to C. verrucosa mediated ZnO NPs.

5. References

1. Nel, A.; Xia, T.; Mädler, L.; Li, N. Toxic potential of materials at the nanolevel. Science **2006**, 311, 622–627.[CrossRef]
2. Mishra, P.K.; Mishra, H.; Ekielski, A.; Talegaonkar, S.; Vaidya, B. Zinc oxide nanoparticles: A promising
nanomaterial for biomedical applications. Drug Discovery Today **2017**, 22, 1825–1834. [CrossRef] [PubMed]
3. Almoudi, M.M.; Hussein, A.S.; Abu Hassan, M.I.; Mohamad Zain, N. A systematic review on antibacterial
activity of zinc against Streptococcus mutans. Saudi Dental J. **2018**, 30, 283–291. [CrossRef] [PubMed]
4. Siddiqi, K.S.; Husen, A.; Rao, R.A.K. A review on biosynthesis of silver nanoparticles and their biocidal
properties. J. Nanobiotechnol. **2018**, 16, 14. [CrossRef] [PubMed]
5. Chen, Y.-H.; Feng, H.-L.; Jeng, S.-S. Zinc Supplementation Stimulates Red Blood Cell Formation in Rats.
Int. J. Mol. Sci. **2018**, 19, 2824. [CrossRef]
6. Nguyen Ly, H.; Tran, T.T.; Thi Ngoc Truong, L.; Mai, H.H.; Nguyen, T.T. Overcharging of the Zinc Ion in
the Structure of the Zinc-Finger Protein is needed for DNA Binding Stability. Biochem **2020**, 59, 1378–1390.[CrossRef]
7. Ruszkiewicz, J.A.; Pinkas, A.; Ferrer, B.; Peres, T.V.; Tsatsakis, A.; Aschner, M. Neurotoxic e_ect of active
ingredients in sunscreen products, a contemporary review. Toxicol. Rep. **2017**, 4, 245–259. [CrossRef]
8. Raghupathi, K.R.; Koodali, R.T.; Manna, A.C. Size-Dependent Bacterial Growth Inhibition and Mechanism of Antibacterial Activity of Zinc Oxide Nanoparticles. Langmuir **2011**, 27, 4020–4028. [CrossRef]
9. Rasmussen, J.W.; Martinez, E.; Louka, P.;Wingett, D.G. Zinc oxide nanoparticles for selective destruction of tumor cells and potential for drug delivery applications. Expert. Opin. Drug Deliv. **2010**, 7, 1063–1077.[CrossRef]
10. Rao, K.M.; Suneetha, M.; Park, G.T.; Babu, A.G.; Han, S.S. Hemostatic, biocompatible, and antibacterial non-animal fungal mushroom-based carboxymethyl chitosan-ZnO nanocomposite for wound-healing applications. Int. J. Biol. Macromol. **2020**, 155, 71–80. [CrossRef]
11. Jiang, Y.; Zhang, L.; Wen, D.; Ding, Y. Role of physical and chemical interactions in the antibacterial behavior of ZnO nanoparticles against E. coli. Mater. Sci. Eng. C **2016**, 69, 1361–1366. [CrossRef]
12. Azizi, S.; Ahmad, M.B.; Namvar, F.; Mohamad, R. Green biosynthesis and characterization of zinc oxide nanoparticles using brown marine macroalga Sargassum muticum aqueous extract. Mater. Lett. **2014**,116, 275–277. [CrossRef]
13. Buzea, C.; Pacheco, I.I.; Robbie, K. Nanomaterials and nanoparticles: Sources and toxicity. Biointerphases **2007**, 2, MR17–MR71. [CrossRef]
14. Padmavathy, N.; Vijayaraghavan, R. Enhanced bioactivity of ZnO nanoparticles—An antimicrobial study. Sci. Technol. Adv. Mat. **2008**, 9, 1–7. [CrossRef] [PubMed]
15. Nair, S.; Sasidharan, A.; Rani, V.D.; Menon, D.; Nair, S.; Manzoor, K.; Raina, S. Role of size

scale of ZnO nanoparticles and microparticles on toxicity toward bacteria and osteoblast cancer cells.
J. Mater. Sci. Mater. Med. **2009**, 20, 235–241. [CrossRef] [PubMed]
16. Heng, B.C.; Zhao, X.; Xiong, S.; Ng, K.W.; Boey, F.Y.; Loo, J.S. Toxicity of zinc oxide (ZnO) nanoparticles on
human bronchial epithelial cells (BEAS-2B) is accentuated by oxidative stress. Food Chem. Toxicol. **2010**, 48, 1762–1766. [CrossRef] [PubMed]
17. Ahamed, M.; Akhtar, M.J.; Raja, M.; Ahmad, I.; Siddiqui, M.K.; AlSalhi, M.S.; Alrokayan, S.A. ZnO
nanorod-induced apoptosis in human alveolar adenocarcinoma cells via p53, survivin and bax/bcl-2
pathways: Role of oxidative stress. Nanomedicine **2011**, 7, 904–913. [CrossRef]
18. Guan, R.; Kang, T.; Lu, F.; Zhang, Z.; Shen, H.; Liu, M. Cytotoxicity, oxidative stress, and genotoxicity in
human hepatocyte and embryonic kidney cells exposed to ZnO nanoparticles. Nanoscale Res. Lett. **2012**, 7, 602. [CrossRef] Molecules **2020**, 25, 4896 18 of 21
19. Goharshadi, E.K.; Abareshi, M.; Mehrkhah, R.; Samiee, S.; Moosavi, M.; Youssefi, A.; Nancarrow, P.
Preparation, structural characterization, semiconductor and photoluminescent properties of zinc oxide
nanoparticles in a phosphonium based ionic liquid. Mat. Sci. Semicon. Proc. **2011**, 14, 69–72. [CrossRef]
20. Moosavi, M.; Goharshadi, E.K.; Youssefi, A. Fabrication, characterization, and measurement of some physicochemical properties of ZnO nanofluids. Int. J. Heat Fluid **2010**, 31, 599–605. [CrossRef]
21. Mason, C.; Vivekanandhan, S.; Misra, M.; Mohanty, A.K. Switchgrass (Panicum virgatum) extract mediated green synthesis of silver nanoparticles. World J. Nano. Sci. Eng. **2012**, 20, 47–52. [CrossRef]
22. Jeevanandam, J.; Chan, Y.S.; Danquah, M.K. Biosynthesis of metal and metal oxide nanoparticles.
Chem. Bio. Eng. Rev. **2016**, 3, 55–67. [CrossRef]
23. Shanker, U.; Jassal, V.; Rani, M.; Kaith, B.S. Towards green synthesis of nanoparticles: From bio-assisted sources to benign solvents. A review. Int. J. Environ. Anal. Chem. **2016**, 96, 801–835.
24. Nagajyothi, P.C.; Minh An, T.N.; Sreekanth, T.V.M.; Lee, J.I.; Joo, D.L.; Lee, K.D. Green route biosynthesis: Characterization and catalytic activity of ZnO nanoparticles. Mater. Lett. **2013**, 108, 160–163. [CrossRef]
25. Nachiyar, V.; Sunkar, S.; Prakash, P. Biological synthesis of gold nanoparticles using endophytic fungi. Der Pharma Chem. **2015**, 7, 31–38.
26. Ramesh, M.; Anbuvannan, M.; Viruthagiri, G. Green synthesis of ZnO nanoparticles using Solanum nigrum leaf extract and their antibacterial activity. Spectrochim. Acta A Mol. Biomol. Spectrosc. **2015**, 136, 864–870.[CrossRef]
27. Rajeshkumar, S. Anticancer activity of eco-friendly gold nanoparticles against lung and liver cancer cells.J. Genet. Eng. Biotechnol. **2016**, 14, 195–202. [CrossRef]
28. Di Carlo, G.; Mascolo, N.; Izzo, A.A.; Capasso, F. Flavonoids: Old and new aspects of a class of naturaltherapeutic drugs. Life Sci. **1999**, 65, 337–353. [CrossRef]
29. Kreft, S.; Knapp, M.; Kreft, I. Extraction of Rutin from Buckwheat (Fagopyrum esculentum Moench) Seeds and Determination by Capillary Electrophoresis. J. Agric. Food Chem. **1999**, 47, 4649–4652. [CrossRef]

30. Azevedo, M.I.; Pereira, A.F.; Nogueira, R.B.; Rolim, F.B.; Brito, G.A.; Wong, D.V.T.; Lima-Júnior, R.C.; De
Albuquerque Ribeiro, R.; Vale, M.L. The antioxidant e_ects of the flavonoids rutin and quercetin inhibit
oxaliplatin-induced chronic painful peripheral neuropathy. Mol. Pain. **2013**, 9, 53. [CrossRef]
31. Gamble, J.S. Flora: Ranunculaceae to Caprifoliaceae. In Flora of the Presidency of Madras, Newman and Adlard 1915 Edition; Authority of the Secretary of State for India: New Delhi, India, 2008.
32. Kumar, S.; Sane, P.V. Legumes of South Asia: A Checklist; Kew Publisher: Kew, UK, 2003.
33. Singh, J. Atlas of Ayurvedic Medicinal Plants; Chaukhambha Sanskrit Bhawan Publisher: Varanasi, India, 2008;
Volume 1.
34. Asolkar, L.V.; Kakkar, K.K.; Charke, O.J. Second Supplement to Glossary of Indian Medicinal Plants with ActivePrinciples. Part-I (A-K) (1965–1981); Publications and Information Directorate (CSIR): New Delhi, India, 1992.
35. Senthilkumar, M.; Gurumoorthi, P.; Janardhanan, K. Some medicinal plants used by Irular, the tribal people
of Marudhamalai hills, Coimbatore, Tamil Nadu. Natural Product Radiance **2006**, 5, 382–388.
36. Rahman, M.A.; Uddin, S.B.;Wilcock, C.C. Medicinal plants used by Chakma tribe in Hill Tracts districts of Bangladesh. Indian J. Tradit. Knowl. **2007**, 6, 508–517.
37. Nwodo, J.N.; Ibezim, A.; Simoben, C.V.; Ntie-Kang, F. Exploring cancer therapeutics with natural products from African medicinal plants, part II: Alkaloids, terpenoids and flavonoids. Anti-Cancer Agents Med. Chem. **2016**, 16, 108–127. [CrossRef]
38. Manokari, M.; Shekhawat, M.S. Role of Crotalaria verrucosa L. extracts in synthesis of Zinc oxide nanoparticles. World Scientific News **2016**, 53, 230–240.
39. Ahmed, Z.S.; Nowrin, T.; Hossain, M.H.; Nasrin, T.; Akter, R. Metabolite profiling of Crotalaria verrucosa leaf extract and evaluation of its antioxidant and cytotoxic potency. Res. J. Phytochem. **2018**, 12, 60–70.
40. Amic, D.; Davidovic-Amic, D.; Beslo, D.; Trinajstic, N. Structure-radical scavenging activity relationships offlavonoids. Croat. Chem. Acta. **2003**, 76, 55–61.
41. Sannigrahi, S.; Mazumder, U.K.; Pal, D.; Mishra, S.L. Hepatoprotective potential of methanol extract of **2009**,5, 394–399.
42. Mahendra, C.; Chandra, M.N.; Murali, M.; Abhilash, M.R.; Brijesh, S.S.; Satish, S.; Sudarshana, M.S.
Phyto-fabricated ZnO nanoparticles from Canthium dicoccum (L.) for Antimicrobial, Anti-tuberculosis and Antioxidant activity. Process Biochem. **2020**, 89, 220–226. [CrossRef] Molecules **2020**, 25, 4896 19 of 21
43. Umar, H.; Kavaz, D.; Rizaner, N. Biosynthesis of zinc oxide nanoparticles using Albizia lebbeck stem bark, and evaluation of its antimicrobial, antioxidant, and cytotoxic activities on human breast cancer cell lines. Int. J. Nanomedicine **2019**, 14, 87–100. [CrossRef]
44. Bharathi, D.; Bhuvaneshwari, V. Synthesis of zinc oxide nanoparticles (ZnO NPs) using pure biofavonoid rutin and their biomedical applications: Antibacterial, antioxidant and cytotoxic activities. Res. Chem. Intermed. **2019**, 45, 2065–2078. [CrossRef]
45. Es-haghi, A.; Soltani, M.; Karimi, E.; Namvar, F.; Homayouni-Tabrizi, M. Evaluation of antioxidant and
anticancer properties of zinc oxide nanoparticles synthesized using Aspergillus niger extract. Mater. Res. Express. **2019**, 6, 125415. [CrossRef]
46. Kanagamani, K.; Muthukrishnan, P.; Saravanakumar, K.; Shankar, K.; Kathiresan, A. Photocatalytic

degradation of environmental perilous gentian violet dye using leucaena-mediated zinc oxide nanoparticle and its anticancer activity. Rare Met. **2019**, 38, 277–286. [CrossRef]
47. Thi, T.D.; Nguyen, T.T.; Dang Thi, Y.; Hanh Ta Thi, K.; ThangPhan, B.; Pham, K.N. Green synthesis of ZnO
nanoparticles using orange fruit peel extract for antibacterial activities. RSC Adv. **2020**, 10, 23899.
48. Malaikozhundan, B.; Vaseeharan, B.; Vijayakumar, S.; Thangaraj, M.P. Bacillus thuringiensis coated zinc oxide nanoparticle and its biopesticidal e_ects on the pulse beetle, Callosobruchus maculates. J. Photochem. Photobiol. B **2017**, 174, 306–314. [CrossRef]
49. Rice-Evans, C.A.; Miller, N.; Paganga, G. Antioxidant properties of phenolic compounds. Trends Plant Sci.**1997**, 2, 152–159
[50] K.J. Klabunde, J. Stark, O. Koper, C. Mohs, D.G. Park, S. Decker, Y. Jiang, I. Lagadic, D. Zhang, Nanocrystals as Stoichiometric Reagents with Unique Surface Chemistry, J. Phys. Chem. 100 (30) (1996) 12142–12153.
[51] V. Nadanathangam, K. Sampath, A.A. Kathe, P.V. Varadarajan, Virendra Prasad, Functional finishing of cotton fabrics using zinc oxide–soluble starch nanocomposites, Nanotechnol. 17 (2006) 5087–5095.
[52] I. Perelshtein, G. Applerot, N. Perkas, E. Wehrschetz-Sigl, A. Hasmann, G.M. Guebitz, A. Gedanken, Antibacterial properties of an in situ generated and simultaneously deposited nanocrystalline ZnO on fabrics, ACS Appl. Mater. Interfaces 2 (2009) 361–366.
[53] L. Zhang, H. Cheng, R. Zong, Y. Zhu, Photo corrosion suppression of ZnO nanoparticles via hybridization with graphite-like carbon and enhanced photo catalytic activity, J. Phys. Chem. C 113 (2009) 2368–2374.
[54] M.M. Abd Elhady, Preparation and characterization of chitosan/zinc oxide nanoparticles for imparting antimicrobial and UV-protection to cotton fabric, J. Carbohydr. Chem. 2012 (2012) 1–6.
[55] A. El, A. Abou-Okeil Shafei, ZnO/carboxymethyl chitosan bionano-composite to impart antibacterial and UV-protection for cotton fabric, Carbohydr. Polym. 83 (2011) 920–925.
[56] S. Karthik, R. Suriyaprabha, K.S. Balu, P. Manivasakan, V. Rajendran, Influence of ball milling on the particles size and antimicrobial property of Tridax procumbens leaf nanoparticles, IET Nanobiotechnol. 11 (2017) 12–17.
[57] A. Edwin Sunder, N.K. Palaniswamy, G. Nalankilli, Protective finishes on cotton textiles using chitosan, Sci. Int. 26 (2) (2014) 709–715.
[58] V. Rajendran, N.R. Dhineshbabu, R.R. Kanna, K.V.I.S. Kaler, Enhancement of thermal stability, flame retardancy, and antimicrobial properties of cotton fabrics functionalized by inorganic nanocomposites, Ind. Eng. Chem. Res. 50 (2014) 19512–19524.
[59] L. Yan, H. Yanyan, Z. Yunling, Microwave assisted fabrication of nano-ZnO assembled cotton fibers with excellent UV blocking property and water-wash durability, Fiber Polym. 13 (2012) 185–190.
[60] R. Rajendran, C. Balakumar, A.M.A. Hasabo, S. Jayakumar, K. Vaideki, E.M. Rajesh, Use of zinc oxide nano particles for production of antimicrobial textiles, Int. J. Eng. Sci. Technol. 2 (2010) 202–208.
[61] A. Elif Selen, U. Husnu Emrah, Zinc oxide nanowire enhanced multifunctional coatings for cotton fabrics, Thin Solid Films 520 (2012) 4658–4661.
[62] P. Nicoleta, E. Monica, Z. Irina, S. Marcela, M. Elena, V. Violeta, E. Ionut, Superhydrophobic properties of cotton fabrics functionalized with ZnO by electroless deposition, Mater. Chem. Phys. 138 (2013) 253–261.

[63] N.F. Attia, M. Moussa, A.M.F. Sheta, R. Taha, H. Gamal, Synthesis of effective multifunctional textile based on silica nanoparticles, Prog. Org. Coat. 106 (2017) 41–49.

THANK YOU